Materials Research Proceedings 31 (2023) 622-633 https://doi.org/10.21741/9781644902592-64

Investigation of the influence of external edge restraint on reinforced concrete walls

Muhammad Kashif Shehzad[1,a*], John P. Forth[1,b], Nikolaos Nikitas[1,c], Imogen Ridley[1,d], Robert Vollum[2,e], Abo Bakr Elwakeel[2,f], Karim El Khoury[2,g], Bassam Izzuddin[2,h]

[1]School of Civil Engineering, University of Leeds, Woodhouse Lane, LS2 9JT, United Kingdom

[2]Imperial College London, Exhibition Rd, South Kensington, London SW7 2BX, United Kingdom

[a]m.k.shehzad@leeds.ac.uk, [b]j.p.forth@leeds.ac.uk, [c]n.nikitas@leeds.ac.uk, [d]cn17ijr@leeds.ac.uk, [e]r.vollum@imperial.ac.uk, [f]a.elwakeel15@imperial.ac.uk, [g]k.khoury20@imperial.ac.uk, [h]b.izzuddin@imperial.ac.uk

Keywords: Edge Restraint, Crack Width, Aspect Ratio, Volume Change, Imposed Strain, Finite Element Analysis

Abstract. Externally restraining volume changes of concrete, i.e., thermal effects and shrinkage, may result in tensile stresses and eventually cracking. Such cracking risk is controlled / mitigated by the provision of steel reinforcement, which presumes correct understanding of the cracking patterns under different types of restraint conditions. Reinforced concrete (RC) members may be restrained at their edges or end, or in many cases a combination of the two. Existing guidance on the subject is mostly based on end restrained members, however it is applied to predict the behaviour under edge restraint too. Researchers have identified that the mechanisms of cracking associated to edge and end restraints are quite different. To this purpose, findings from an experimental investigation aiming to understand the behaviour of edge restrained RC walls were utilized to validate a finite element (FE) model. Subsequently, this FE model was used to study the edge restrained walls having different aspect ratios. Cracking patterns, widths and extent appeared to greatly depend on the wall aspect ratio. The study provides clear evidence on why similar studies related to all forms of restraint are needed to support engineers in designing against cracking due to restraints.

Introduction

The design of members subjected to restraint of imposed strains has traditionally been based on the principles of end restraint i.e., members fully restrained at both ends [1]. Whilst appropriate for elements subjected to end restraint, this is wholly inappropriate for members subjected to edge restraint as each restraint mechanism produces totally different cracking patterns and mechanisms [2]. For instance, for end restraint: 1) the restraint is uniform throughout and when a crack occurs, stress in the entire member is relieved; 2) the crack can occur anywhere along the length of the member depending mainly on the variation of the concrete tensile strength; 3) a crack, when formed, reaches its maximum width before another new crack forms. Whereas, for edge restraint: it is not uniform; it is maximum at the base and reduces over the height of the member; stress relief upon cracking is local to the area around crack, and the variation in edge restraint depends on the ratio of length to height (L/H), the location of the restraint within the member, the roughness of the concrete surface (between the restraining and the restrained panel) and the wall and base dimensions [3, 4].

Knowledge of the likely cracking patterns is essential while deciding on the steel reinforcement. Not much guidance on the cracking patterns in RC members under restraint exists. Typical cracking patterns for restrained members are proposed in Annex L to BS EN 1992-3 [5] (see Fig.1).

According to this guidance, no crack is formed within 2.4 m from the free ends of the wall (9, 10), however Al-Rawi [6] suggested that no crack would form within a distance equal to the wall height, from the free end. ACI Committee 207 [7] describes the method of estimation of degree of restraint but does not provide any guidance on the location and orientation of the cracks under different types of restraint.

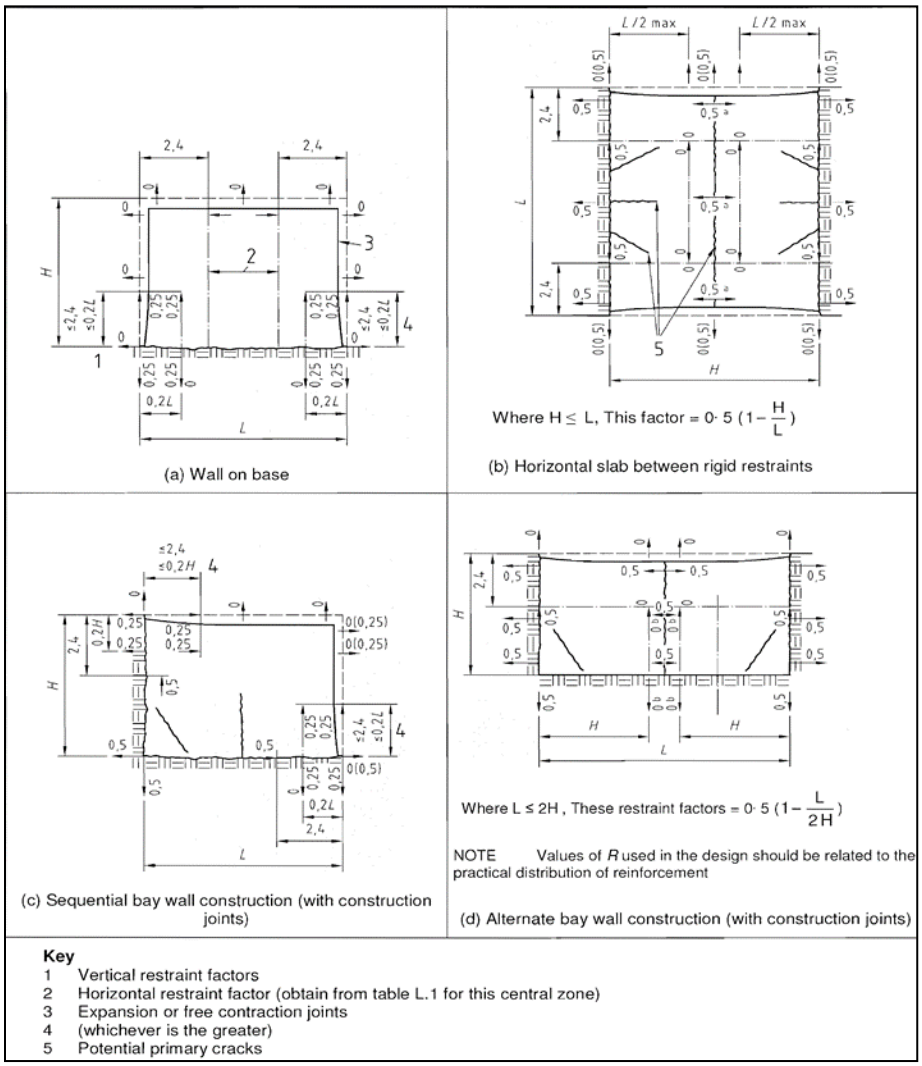

Fig. 1: Illustration of cracking patterns for members under various types of restraint [5]

Although two types of restraint i.e. End and Edge restraint are defined and considered separately, however in practice, the situation is likely to be more complex and restraint of the newly cast member may be a combination of edge and end restraint. An example of a situation where both forms of restraint may exist can be found by considering a new section of concrete cast between two pre-existing concrete wall sections and onto a pre-existing concrete base [9]. Whilst a greater understanding of edge restraint in isolation is being gained [10, 11], the optimum problem constituted by a combination of the two restraints is still little understood. Forth [12] suggested that in such a scenario, both types of restraint will dominate in different parts of the wall. Edge restraint will be dominant closer to the base, however, moving further up from the base, the effect of edge restraint will get less significant, and the influence of end restraint becomes more pronounced. At a point within the height of the wall, end restraint becomes dominant and edge restraint becomes insignificant. As part of the ongoing EPSRC UK funded research being

Materials Research Proceedings 31 (2023) 622-633 https://doi.org/10.21741/9781644902592-64

conducted jointly at the University of Leeds and Imperial College London, the combined restraint is being investigated experimentally to confirm the above distribution of restraint in RC members.

This paper presents an experimental study which was purposefully designed [11] to understand the behaviour of RC walls when their imposed strains are subjected to edge restraint. Findings from this experimental investigation are utilized to validate a finite element (FE) model, which is used to study walls having different aspect ratios and subjected to external edge restraint.

Experimental Investigation

An experimental study of RC walls restrained along their edge has been undertaken at the University of Leeds, UK. As part of this experimental investigation, four walls were tested, and each test continued for a period of 12 weeks. In each test, a RC wall was cast onto an already cast and hardened RC base. Initially, the RC base slab was cast and cured for up to 14 days. Subsequently, once the slab was at least 28 days old, the wall was cast on it; hence, the existing slab imposed a restraint to the volume changes occurring in the newly cast wall. The walls had an aspect ratio (L/H) of 4, which is representative of the upper values of commonly used aspect ratios in practice. The ratio of vertical steel reinforcement was varied for each test, i.e., 0.07%, 0.9%, 0.1% and 1.4% in tests 1, 2, 3 and 4, respectively. This was done to evaluate the influence of vertical steel on the degree of restraint [11]. Moreover, the wall thickness was 300 mm in test 1 and 2 but was reduced to 200 mm in tests 3 and 4. The heights of the base and the wall were, however, kept constant during all the tests as 300 mm and 800 mm, respectively. Thus, in the first two tests the walls had a larger cross-sectional area (240000 mm^2) than that of the base slab (204000 mm^2) whereas in the last two tests, the cross-sectional area of the walls (160000 mm^2) was less than that of the base slab (204000 mm^2). This enabled the influence of relative cross-sectional areas on the degree of restraint to be established. The geometric and reinforcement details of the tested specimens are given in Fig. 2 and a pictorial illustration of test 4 is given in Fig. 3.

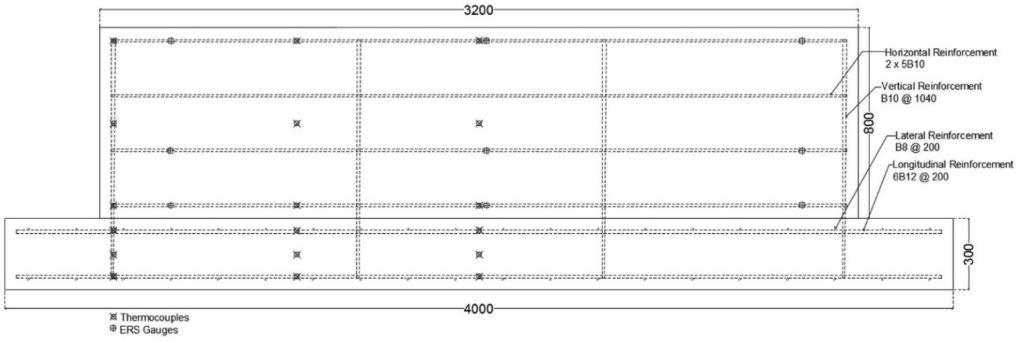

(a)

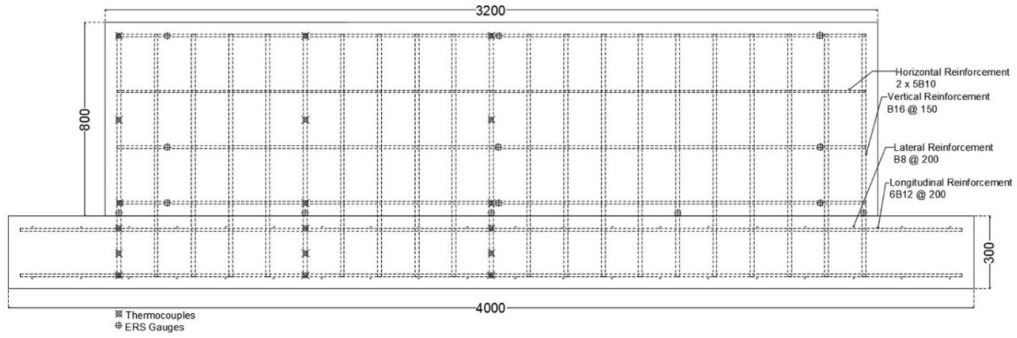

(b)

Fig. 2: Geometric and reinforcement details of tested walls: (a) Test 1 & 3; (b) Test 2 & 4 (all dimensions in mm)

Materials Research Proceedings 31 (2023) 622-633 https://doi.org/10.21741/9781644902592-64

Fig. 3: Illustration of the experimental work setting

Temperature development in both the wall and slab was monitored using welded tip Type K thermocouples. The temperature profiles recorded during each test are presented in Fig. 4. The vertical dotted lines in Fig. 4(b) depict the time that the formwork was removed. A sharp decline in temperature can be seen in all tests on removal of the formwork. Temperatures within the concrete dropped to ambient values after 72 to 80 hours from initial casting and the temperature drop remained gradual except at the time of formwork removal. The maximum temperatures observed in tests 1, 2, 3 and 4 were 55.4°C, 50.5°C, 48.8°C and 42.2°C, respectively; these values occurred near the top of the wall along the wall centerline. Temperatures observed in the wall close to the joint between the wall and the base were significantly lower than those at the higher locations in the wall due to flow f heat into adjoining base slab. The temperature drop (T_1) from the peak to the ambient temperature was 33.5°C in test 1, 33.3°C in test 2, 25.4°C in test 3 and 25°C in test 4 which compare reasonably well with the values predicted by CIRIA C766 [8].

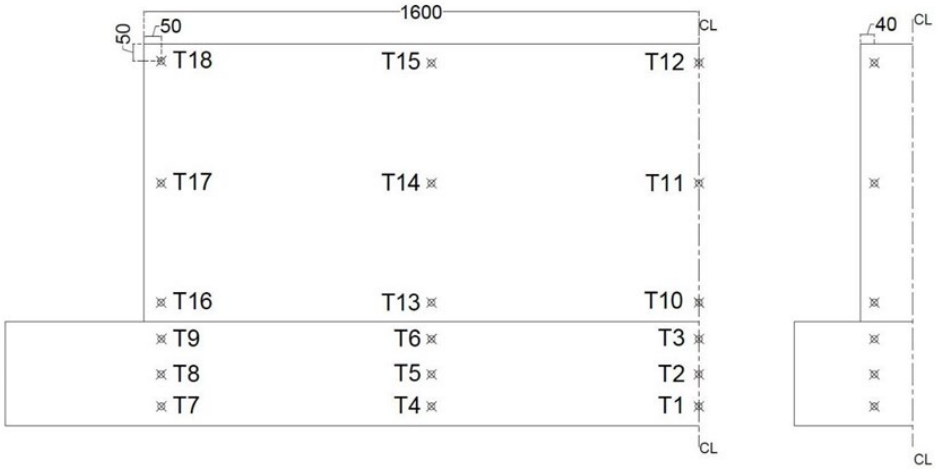

(a)

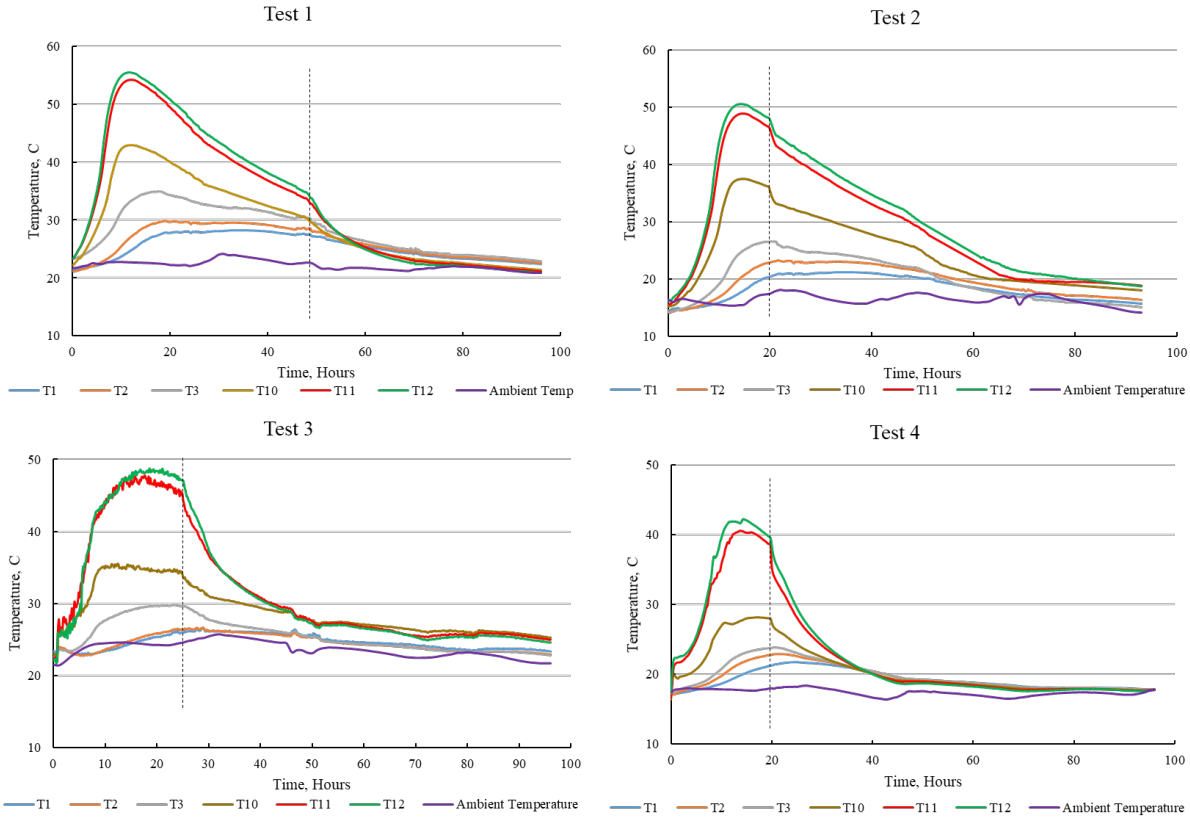

(b)

Fig. 4: Temperature profile observed in base slab and wall: (a) location and naming of thermocouples (all dimensions in mm); (b) temperature profile at mid-section, for different tests.

The strain occurring at the surface of the concrete wall and base was monitored using demountable mechanical gauges (DEMECs). In terms of edge restraint, the middle of the wall was considered to be the most critical section and as such, a 150 mm DEMEC gauge was used in the central one third of the walls; and a 400 mm gauge length was used towards the ends. Strain monitoring on the walls commenced within two hours after removal of the formwork. The free strain of the base and wall elements was equivalent to the summation of the unrestrained shrinkage and thermal strain of the concrete. The unrestrained shrinkage for each batch of concrete was obtained from small prisms, cast from the concrete used to make the base and wall elements and which were monitored throughout the duration of the tests. A comparison between the predicted and measured shrinkage revealed that the experimentally obtained shrinkage profiles from the prisms were most accurately predicted using the fib Model code 2010 [13]. Thermal strain was calculated using the temperature profiles (Fig.4) and a coefficient of thermal expansion of concrete equal to 10 microstrain per degrees C [13, 14]. By subtracting the measured strains from the free or unrestrained strain, the restrained strain could be calculated. The degree of restraint was then determined as the ratio of restrained to free strain. The restraint values obtained during each test were compared to those calculated using the methods available in both ACI and the Eurocode as well as to those worked out by Schleeh [15]. The restraint profiles obtained at the 7th and last day of each test are given in Fig. 5. It is evident that the degree of restraint calculated using the various methods is very different to the values which were obtained during this experimental investigation. The steel reinforcement continuing from restrained to restraining member has been identified as a key influencing factor for this variation. No account of this important factor is made in the current

Materials Research Proceedings 31 (2023) 622-633 https://doi.org/10.21741/9781644902592-64

guidance for determination of the degree of restraint. This suggests the need to develop a more accurate methodology for the estimation of the degree of restraint.

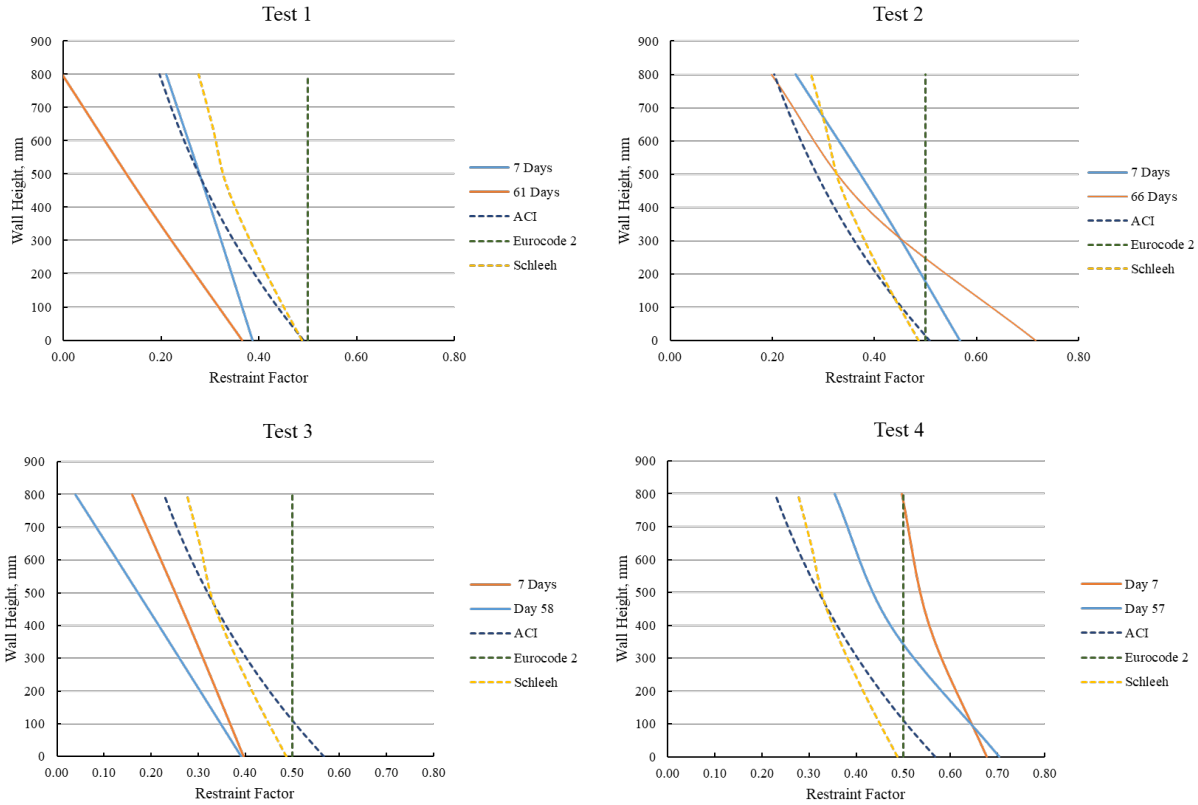

Fig. 5: Edge restraint profiles and their comparison with available estimation methods.

Finite Element (FE) Analysis

As part of this research, the FE models of the experimentally tested walls developed using MIDAS FEA (a commercially available FE based software), were prepared, and validated (7) prior to extending the parameter space. The FE study was undertaken by performing 3D nonlinear and linear analysis using MIDAS FEA. The material properties and the thermal strain and shrinkage obtained from the experimental study were used as input data for the models. The FEA study investigated walls with aspect ratios 1, 2, 4, 6 and 12 subjected to external edge restraint. The dimensions of the restraining concrete members and the restrained walls are presented collectively in Table 1. Taking advantage of the symmetry of the specimens, the reinforcement, loading and boundary conditions, a quarter of the wall and base elements were modelled.

Table 1: Geometric dimensions of restrained and restraining members.

Dimensions [m]	Restraining Slab	Restrained Wall
Length	15	12
Thickness	1	0.4
Height	0.5	1, 2, 3, 6, 12

The material properties of the concrete and steel obtained during the experimental study, given in Table 2, were used and concrete was modelled using the Total strain crack model [16]. Since the restrained contraction induces tension and ultimately results in cracking of the concrete, modelling of the tensile behaviour of concrete accurately is of great significance for the ensuing

Materials Research Proceedings 31 (2023) 622-633 https://doi.org/10.21741/9781644902592-64

analysis. In this case, the nonlinear behaviour of concrete in tension was modelled using the Hordijk model [17]. Concrete was modelled using 3D solid elements. After performing a mesh sensitivity analysis, and carefully considering the balance between computing effort and the effect of mesh size on the results, mesh size for the restraining elements was selected as 100 mm. The reinforcement was modelled as fully embedded bar in a solid hence the stiffness of the reinforcement elements is added to the surrounding concrete elements [16]. The wall reinforcement detail was as follows: 12 mm bars spaced at 200 mm in the horizontal direction, along both faces; 16 mm bars spaced at 150 mm in the vertical direction. The area of steel provided was, therefore, 1130 mm^2/meter and 2680 mm^2/meter in the horizontal and vertical directions, respectively.

Table 2: Material properties of concrete and steel

Material Properties	**Restraining Members**	**Restrained Wall**
Compressive Strength, f_{cm} [Mpa]	43.3	31.0
Tensile Strength, f_{ctm} [Mpa]	3.4	2.4
Modulus of Elasticity, E_c [Mpa]	31000	24500
Coefficient of thermal expansion, α [με / ℃]	10	10
Poisson Ratio, γ	0.18	0.16
Fracture Energy, G_f [N/mm]	0.143	0.135
Thermal Conductivity, k [W/m]	1.76	2.03
Specific Heat, c [KJ/Kg C]	0.95	0.74
Steel Yield Strength, f_y [Mpa]	460	460

The end nodes of the base slab were constrained for translation along all three directions. Respective constraints were also applied along the symmetrical faces of the models for each case. Due to the limitations of the software, shrinkage could not be applied simultaneously with the thermal strain, therefore, the thermal strain and shrinkage was simulated by applying an equivalent thermal contraction, which represented the thermal strain and shrinkage, to the wall elements. It was noticed from the experimental investigation and also from the findings of other researchers [9, 18], that the thermal strain in the wall is lower adjacent to the restraining element and at the free edges of the member. Accordingly, the imposed thermal strain applied to the models was varied along the length and height of the wall. The nonlinear analysis was performed using the Newton Raphson solution technique. Force and Energy Norms for the convergence criteria, with a tolerance level of 0.001 for both norms, were specified in the iterative solution.

Results and Discussion

From the analysis, it was identified that the tensile stress in the restrained member increases with the increase in equivalent thermal contraction, until a crack occurs. On occurrence of cracking, the stress in the vicinity of the crack drops and contraction further increases. The stress in the remaining member, away from the crack, continues to increase until a second crack forms; again, this second crack relieves the stress in its vicinity. This pattern of crack formation and localized stress relief is in line with the guidance provided by Bamforth [8] in CIRIA C766. Observation of the stress development in the members also indicated that as the wall height increased, less stress developed close to the free edges, mainly because of the absence of restraint in those parts. This phenomenon prevented the propagation of the cracks to the top of the wall and to the free ends, however, this was only noticed in walls with an aspect ratio of less than 2.

Materials Research Proceedings 31 (2023) 622-633 https://doi.org/10.21741/9781644902592-64

The cracking sequence and patterns for all wall aspect ratios were obtained from the strain profiles. The variation of strains in the wall clearly indicates the initiation and propagation of the cracks. The sequence in which the cracks appeared was noted and the cracks were accordingly numbered (see Figs. 6 to 10). One half of the wall was modelled due to symmetry along length. The location of the maximum crack width, which was obtained from the analysis, is also marked on the figures with a red circle.

L/H - 12: First crack appeared close to the centerline, indicated by the circled 1, of the wall and the cracking pattern indicates that all of the cracks propagated vertically and reached the top of the wall (Fig. 6). The location of the maximum crack width in the wall occurred at 900mm (8% of the wall length) above the base.

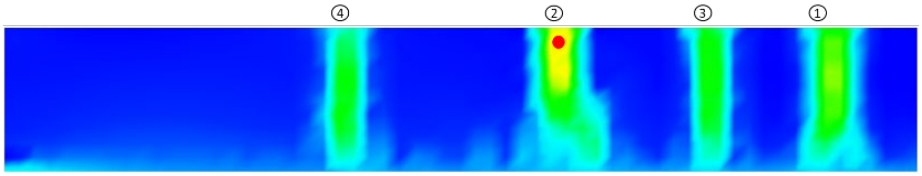

Fig. 6: Cracking patterns and marked sequences for wall with L/H 12

L/H - 6: In the case of wall with aspect ratio 6, the first crack appeared close to the center of the wall and most of the cracks reached to the top of the wall (Fig. 8). The number of cracks is the same as found in the edge restrained wall with an aspect ratio of 12. All cracks initiated at the base and propagated upwards, mostly remaining vertical. No significant cracking was seen within the zone of no cracking specified in the Annexure L of BS EN 1992-3. The location of the maximum crack width occurred close to the wall top, 1500mm (13% of the wall length) above the base.

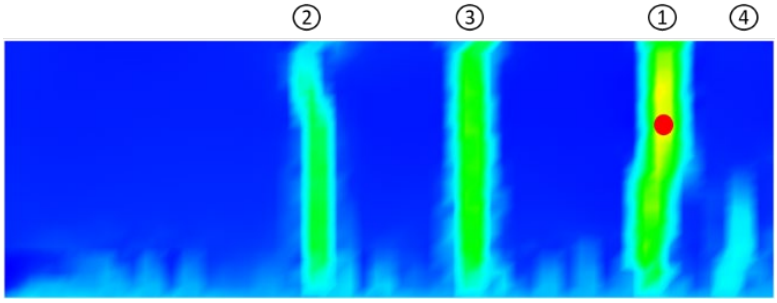

Fig. 7: Cracking patterns and marked sequences for wall with L/H 6

L/H - 4: The first crack still appeared close to the center of the wall and reached the full height of the wall (Fig. 8). None of the other cracks appearing subsequently reached the top of the wall. The cracks appearing in the outer one third of the wall length were inclined towards the free ends and prominent cracking was seen close to the end of the wall, within 2.4m of the end which is contrary to the specification of BS EN 1992-3. In this case, the maximum crack width occurred 1200mm (10% of the wall length) above the base.

Materials Research Proceedings 31 (2023) 622-633 https://doi.org/10.21741/9781644902592-64

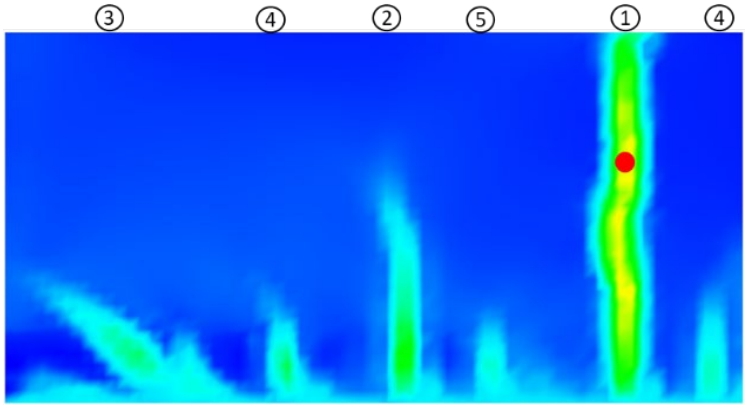

Fig. 8: Cracking patterns and marked sequences for wall with L/H 4

L/H - 2: The results suggest that when the aspect ratio of wall is reduced to 2, the cracking patterns are considerably different to their equivalents in higher aspect ratio walls. The first crack in the edge restrained wall (Fig. 9) appeared close to the center and reached the maximum height among all other cracks at this location, however, no crack reached the top of the wall. The cracks were inclined as they propagated and a noticeable amount of cracking close to the free edge was observed. The maximum crack width occurred 800 mm (7% of the wall length) above the base.

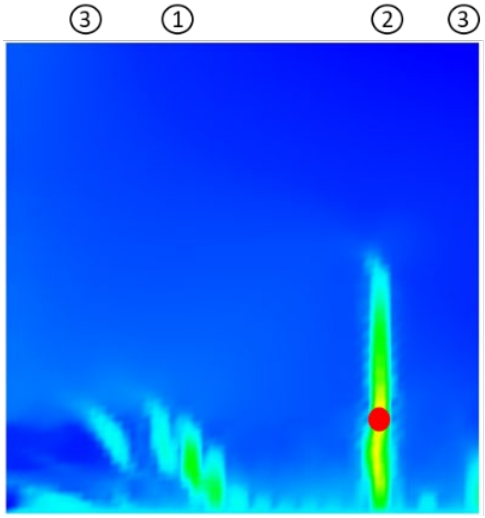

Fig. 9: Cracking patterns and marked sequences for wall with L/H 2

L/H - 1: The cracking behaviour of these walls again continued to deviate from the behaviour of the walls with aspect ratios greater than 2. The first crack, in Fig. 10, appeared at the center of the wall and propagated to approximately one third of the wall height. Subsequent cracks were less in height and did not propagate vertically but were inclined at different angles. The maximum crack width appeared 1800 mm (15% of the wall length) above the base. Although a number of cracks appeared, none of the cracks spanned the entire height of the wall.

Fig. 10: Cracking patterns and marked sequences for wall with L/H 1

As indicated above, the initiation and propagation of the cracks in the walls, as well as the location of the maximum crack width varies. It was also noticed that when a new crack was formed, the width of the existing cracks, in some instances, often decreased. The maximum crack widths for each wall examined in this study are summarized in Table 3. Crack width for the considered wall dimensions and steel reinforcement was also calculated according to BS EN 1992-3 and was found to be 0.249 mm. In all cases the maximum crack width was found to be significantly higher than the calculated value. As explained above, the location of the maximum crack width in the case of edge restraint lies at a height above the base, which in the considered cases varied from 7-15% of the wall length. This slightly differs from the findings of other researchers [6, 8] who found the location of maximum crack width to be at a height equal to 10-12% of the wall length.

Table 3: Maximum crack width for each aspect ratio

Aspect Ratio	Maximum Crack Width (MCW) [mm]	Location of MCW above base [mm]
12	0.516	900
6	0.672	1800
4	0.493	1400
2	0.480	900
1	0.689	1900

Conclusions

Results from the experimental and FE based investigation of the influence of edge restraint on the behaviour of reinforced concrete walls have been presented and discussed. The location of cracks in the region of the free ends, particularly in the case of edge restraint alone, indicates that the 'No crack zone' proposed in the Eurocode is not always correct. It is observed that in walls with aspect ratios of less than 6, significant cracking can occur close to the free end. Formation of a crack results in localized relief in stress and formation of another crack in the member at a point where the stress level remained unaffected. In higher walls, the cracks due to edge restraint do not reach the full height of the wall. With an increase in the wall height (i.e. decrease in aspect ratio), the number of cracks appearing in the wall decreases.

Acknowledgements
The authors kindly acknowledge financial support from the Engineering and Physical Sciences Research Council (EPSRC) UK, under grants EP/T004142/1 and EP/T004185/1 titled Understanding the cracking behaviour of reinforced concrete elements subjected to the restraint of imposed strains.

References

[1] E. Evans and B. Hughes, "SHRINKAGE AND THERMAL CRACKING IN A REINFORCED CONCRETE RETAINING WALL," in ICE Proceedings, 1968, vol. 39, no. 1, pp. 111-125: Thomas Telford. https://doi.org/10.1680/iicep.1968.8172

[2] J. P. Forth, A.J. Martin, Design of Liquid Retaining Concrete Structures, Third ed. UK: Whittles Publishing, 2014, p. 175.

[3] H. Stoffers, Cracking due to shrinkage and temperature variation in walls. Stevin Laboratory, Department of Civil Engineering, Delft University of Technology and IBBC Institute TNO for Building Materials and Building Structures, 1978.

[4] G. Kheder and R. Al Rawi, "Control of cracking due to volume change in base-restrained concrete members," ACI Structural Journal, vol. 87, no. 4, 1990. https://doi.org/10.14359/2747

[5] BS EN 1992-3, Eurocode 2: Design of Concrete Structures: Part 3: Liquid retaining and containment structures. British Standards Institution, 2006.

[6] G. Kheder, R. Al-Rawi, and J. Al-Dhahi, "A study of the behaviour of volume change cracking in base restrained concrete walls," Materials and Structures, vol. 27, no. 7, pp. 383-392, 1994. https://doi.org/10.1007/BF02473441

[7] ACI Committee 207, "Effect of restraint, volume change, and reinforcement on cracking of mass concrete," ACI Materials Journal, vol. 87, no. 3, 2007.

[8] P. Bamforth, Control of cracking caused by restrained deformation in concrete. CIRIA, 2018.

[9] M. Micallef, Vollum, RL, Izzuddin, BA, "Crack development in transverse loaded base-restrained reinforced concrete walls," Engineering Structures, vol. 143, pp. 522-539, 2017. https://doi.org/10.1016/j.engstruct.2017.04.035

[10] M. Micallef, R. L. Vollum, and B. A. Izzuddin, "Cracking in walls with combined base and end restraint," Magazine of Concrete Research, vol. 69, no. 22, pp. 1170-1188, 2017. https://doi.org/10.1680/jmacr.17.00026

[11] M. K. Shehzad, J. P. Forth, and A. Bradshaw, "Imposed Loading Effects on Reinforced Concrete Walls Restrained at Their Base," Proceedings of the Institution of Civil Engineers-Structures and Buildings, pp. 1-29, 2018.

[12] J. P. Forth, "Chapter 7 Edge Restraint, The Concrete Society Technical Report No 67," in "Accommodating Movement in Concrete Structures," 2008.

[13] Fib model code for concrete structures 2010, 2010.

[14] BS EN 1992-1-1, Eurocode 2: Design of Concrete Structures: Part 1-1: General Rules and Rules for Buildings. British Standards Institution, 2004.

[15] W. Schleeh, "Imposed stresses in the walls one-side restrained," Beton- Und Stahlbetonbau, vol. 57, no. 3, pp. 64-72, 1962.

[16] F. Midas, MIDAS FEA: Analysis and Algorithm (Advanced Nonlinear and Detailed Analysis System). MIDAS IT, 1989.

[17] D. A. Hordijk, Local approach to fatigue of concrete. TU Delft, Delft University of Technology, 1991.

[18] B. Klemczak and A. Knoppik-Wróbel, "Analysis of Early-Age Thermal and Shrinkage Stresses in Reinforced Concrete Walls (with Appendix)," ACI Structural Journal, vol. 111, no. 2, 2014. https://doi.org/10.14359/51686523